Elastomers and Composites
Vol. 55, No. 3, pp. 191~198 (September 2020)

Print ISSN 2092-9676/Online ISSN 2288-7725
DOI: https://doi.org/10.7473/EC.2020.55.3.191

Catalytic Reduction of *ortho*- and *meta*-Nitroaniline by Nickel Oxide Nanoparticles

Sugyeong Jeon[*], Jeong Won Ko[**], and Weon Bae Ko[*, **, *,†]**

[*]*Department of Convergence Science, Graduate School, Sahmyook University, 815, Hwarang-ro, Nowon-gu, Seoul 01795, Republic of Korea*
[**]*Nanomaterials Research Institute, Sahmyook University, 815, Hwarang-ro, Nowon-gu, Seoul 01795, Republic of Korea*
[***]*Department of Chemistry, Sahmyook University, 815, Hwarang-ro, Nowon-gu, Seoul 01795, Republic of Korea*

(Received July 14, 2020, Revised July 27, 2020, Accepted August 2, 2020)

Abstract: Nickel oxide (NiO) nanoparticles were synthesized by a reaction of nickel nitrate hexahydrate ($Ni(NO_3)_2 \cdot 6H_2O$) and sodium hydroxide (NaOH). The synthesized NiO nanoparticles were examined with X-ray diffraction, scanning electron microscopy, Raman spectroscopy, and ultraviolet-visible (UV-vis) spectroscopy. The NiO nanoparticles were used as the catalyst for the reduction of *o*- and *m*-nitroaniline to phenylenediamine. The reduction rate of *m*-nitroaniline was faster than that of *o*-nitroaniline. The reduction rate for both *o*- and *m*-nitroaniline increased as the reaction temperature increased. The rate of reduction for nitroaniline followed a pseudo first-order reaction rate law.

Keywords: Catalytic reduction, Nickel oxide nanoparticles, *o*-Nitroaniline, *m*-Nitroaniline

Introduction

Nitroanilines are used as intermediates in pharmaceuticals, pesticides, pigments, dyes, and rubber chemicals.[1] They are toxic contaminants in viewpoint of the environment. The nitro anion radicals are known as mutagens and carcinogens. They disturb biochemical cycles and their effects are consequently observed in nature.[1] Therefore, effective methods to remove nitroanilines from industrial wastewater are necessary. The types of nitroaniline include ortho-, meta-, and para-nitroaniline, depending on the location of the nitro functional group. Various methods for nitroaniline removal, such as adsorption, thermal decomposition, photocatalysis, biological degradation, and catalytic reduction, have been investigated.[2–4]

The most favored method of nitroaniline removal is catalytic reduction in an aqueous solution because the products of catalytic reductions are applied in various fields.[3] The organic compound *m*-phenylenediamine is used as a raw material for a polymer synthesis such as polyurea elastomers, which are included as dye elements in the textile industry.[3] *o*-Phenylenediamine is used as a precursor in pharmaceuticals, dyes, and antiseptic agents. Therefore, the catalytic reduction of nitroaniline to phenylenediamine is preferred over the other methods.[5]

Nickel oxide (NiO) is a type of important semiconducting material. It has been extensively used in various fields, including capacitors, rechargeable lithium-ion batteries, gas-sensing material, and catalysis.[6,7] The photocatalytic efficiency of NiO nanoparticles was confirmed by researching the photodegradation of methylene blue.[8,9] Nickel oxide nanoparticles are synthesized through various methods including the sol-gel method, microwave, hydrothermal method, sonochemical synthesis, and precipitation method.[6,10–14]

In this work, we studied the catalytic reduction of *o*- and *m*-nitroaniline from an aqueous solution using NiO nanoparticles as catalyst.

Experimental

1. Chemicals

Nickel nitrate hexahydrate ($Ni(NO_3)_2 \cdot 6H_2O$), sodium hydroxide (NaOH), *o*-nitroaniline ($H_2NC_6H_4NO_2$) and *m*-nitroaniline ($H_2NC_6H_4NO_2$) were purchased from SAMCHUN PURE CHEMICALS and Sigma-Aldrich, Merck. Deionized water was

†Corresponding author E-mail: kowb@syu.ac.kr

used as the dispersing solvent.

2. Instruments

X-ray diffraction (XRD) analysis of the samples were carried out using an X-ray diffractometer (Bruker, D8 ADVANCE) with Cu Kα (1.5406 Å) radiation in the range of $10^{o}-90^{o}$. The morphology of the samples was characterized by scanning electron microscopy (SEM) (JEOL Ltd, JSM-6510) at an acceleration voltage of 10 kV. The chemical structure phase of the sample was investigated by Raman spectroscopy (BWTEK, BWS465-532S).

3. Synthesis of NiO nanoparticles

NiO nanoparticles were synthesized using the co-precipitation method described as follows. First, 0.2 M nickel nitrate hexahydrate ($Ni(NO_3)_2 \cdot 6H_2O$, 0.872 g) and 0.4 M sodium hydroxide (NaOH, 0.24 g) were dissolved in 15 ml of distilled water, respectively. Then, sodium hydroxide solution was mixed with drop wise in aqueous nickel nitrate solution under stirring condition. After the reaction was performed, the green precipitate was obtained and washed several times with distilled water and dried in an oven at 100°C. The green precipitate ($Ni(OH)_2$) was heated in an electric furnace under Ar gas at 400°C for 1 h. The color of the precipitate powder turned from green to black.[8,15]

4. Catalytic reduction of *o*- and *m*-nitroaniline in the presence of $NaBH_4$ by nickel oxide nanoparticles

The catalytic reduction of o- and m- nitroaniline by nickel oxide nanoparticles was carried out in the presence of $NaBH_4$. The initial concentration of *o*- and *m*-nitroaniline solutions was 1.45×10^{-2} mM. 13.4 mM of $NaBH_4$ was added to 1.45×10^{-2} mM of *o*- and *m*-nitroaniline solutions, respectively.

5 mg of NiO nanoparticles were added to *o*- and *m*-nitroaniline solutions and stirred using a magnetic stirrer. The catalytic reduction of *o*- and *m*-nitroaniline was measured with every 10 min interval by UV-vis spectroscopy.

Table 1. Average Crystallite Size of Nickel Oxide Nanoparticles Evaluated Using the Scherrer Equation

Miller Indices (*hkl*)	Diffraction angle 2θ (degree)	Full width at half maximum (degree)	Average crystallite size (nm)
(111)	37.335	0.323	
(200)	43.381	0.333	
(220)	63.022	0.435	20.58
(311)	75.600	0.510	
(222)	79.607	0.526	

Results and Discussion

The XRD patterns of NiO were observed at $2\theta = 37.30^{o}$, 43.33^{o}, 62.94^{o}, 75.48^{o}, and 79.49^{o} corresponding to the (111), (200), (220), (311), and (222) planes of the cubic phase, respectively (Figure 1). The crystallite size of synthesized NiO nanoparticles was calculated using the Scherrer formula[16]:

$$D = \frac{k\lambda}{\beta \cos\theta}$$

D is the crystallite size of synthesized NiO nanoparticles,

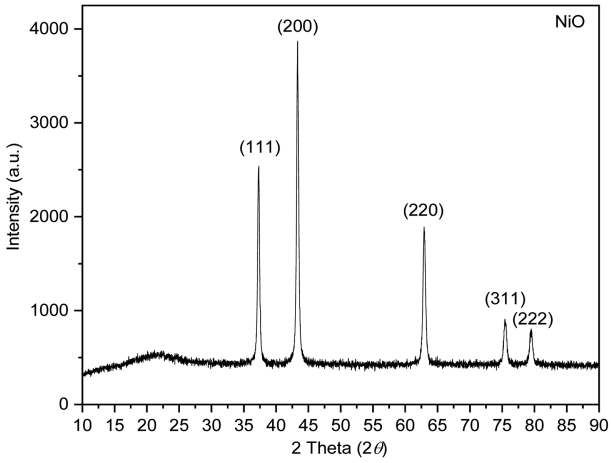

Figure 1. XRD pattern of the synthesized NiO nanoparticles.

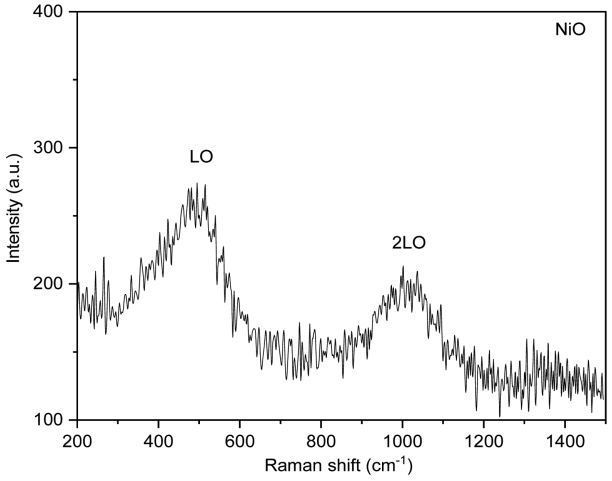

Figure 2. Raman spectrum of the synthesized NiO nanoparticles.

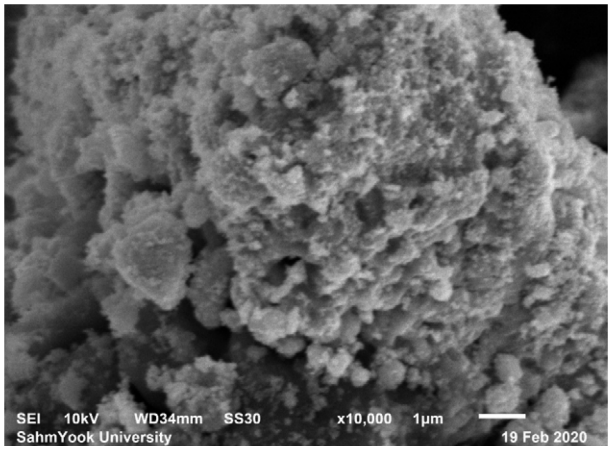

Figure 3. SEM image of the synthesized NiO nanoparticles.

k is the Scherrer constant (0.89), λ is the X-ray wavelength, β is the full width at half maximum (FWHM) of the X-ray diffraction peak, and θ is the Bragg angle. The average crystallite size of the NiO nanoparticles was calculated to be 20.58 nm (Table 1).[17]

The Raman spectrum of NiO nanoparticles show one-phonon LO mode and two-phonon 2LO modes. Defects of the lattice produced phonon scattering in a single crystal.[18] The peak value of 514.73 cm^{-1} corresponds to LO due to first-order scattering, the peak value of 1036.47 cm^{-1} is attributed to 2LO due to second-order scattering (Figure 2).[19]

The morphology of NiO nanoparticles was investigated by SEM. The SEM image of the NiO nanoparticles revealed that they are oval-shaped particles (Figure 3).[8]

The change of nitroaniline concentration was monitored over time by UV-vis spectroscopy. The synthesized NiO nanoparticles was used as the reduction catalyst of *o*- and *m*-nitroaniline to *o*- and *m*-phenylenediamine with $NaBH_4$ reducing agent. The *o*-nitroaniline was added into deionized water. The color of solution was yellow and the peaks of the UV-visible spectrum of the *o*-nitroaniline solution appeared at 283 and 412 nm. The absorption peak at 283 nm shifted to a longer wavelength at 289 nm and the absorption peak at 412 nm disappeared (Figure 4a).[3] The UV-visible spectrum of *m*-nitroaniline appears at 280 and 358 nm. The absorption peak at 280 nm shifted to a longer wavelength at 289 nm and the absorption peak at 358 nm disappeared (Figure 4b).

The catalytic activities occurred due to the hydrogen generation between the $NaBH_4$ and water molecules on the catalytic surface.[20] Borohydride ions was generated on the surface of the NiO nanoparticles. At the same time, nitroaniline molecules were adsorbed on the surface of the NiO nanoparticles. After

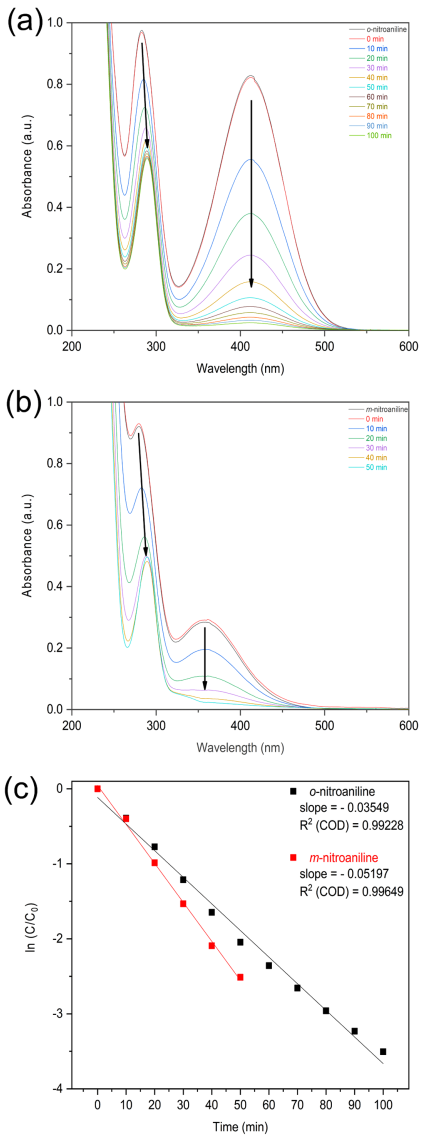

Figure 4. UV-vis absorption spectra for the reduction and kinetic study of (a) *o*-nitroaniline (b) *m*-nitroaniline and (c) their kinetic study at 40°C of *o*-nitroaniline and *m*-nitroaniline in the presence of $NaBH_4$ with NiO nanoparticles as catalyst.

adsorption on the catalytic surface, nitroaniline was reduced to phenylenediamine by the transfer of hydrogen from BH_4^- ions to the NO_2 group of nitroaniline.[21,22]

Since the concentration of $NaBH_4$ in the reaction is higher than that of nitroaniline, it is possible to assume that the concentration of sodium borohydride remains constant during the reduction reaction. The reduction follows a pseudo-first order reaction rate law (Figure 4c).[23]

$$\frac{dc}{dt} = -kC$$

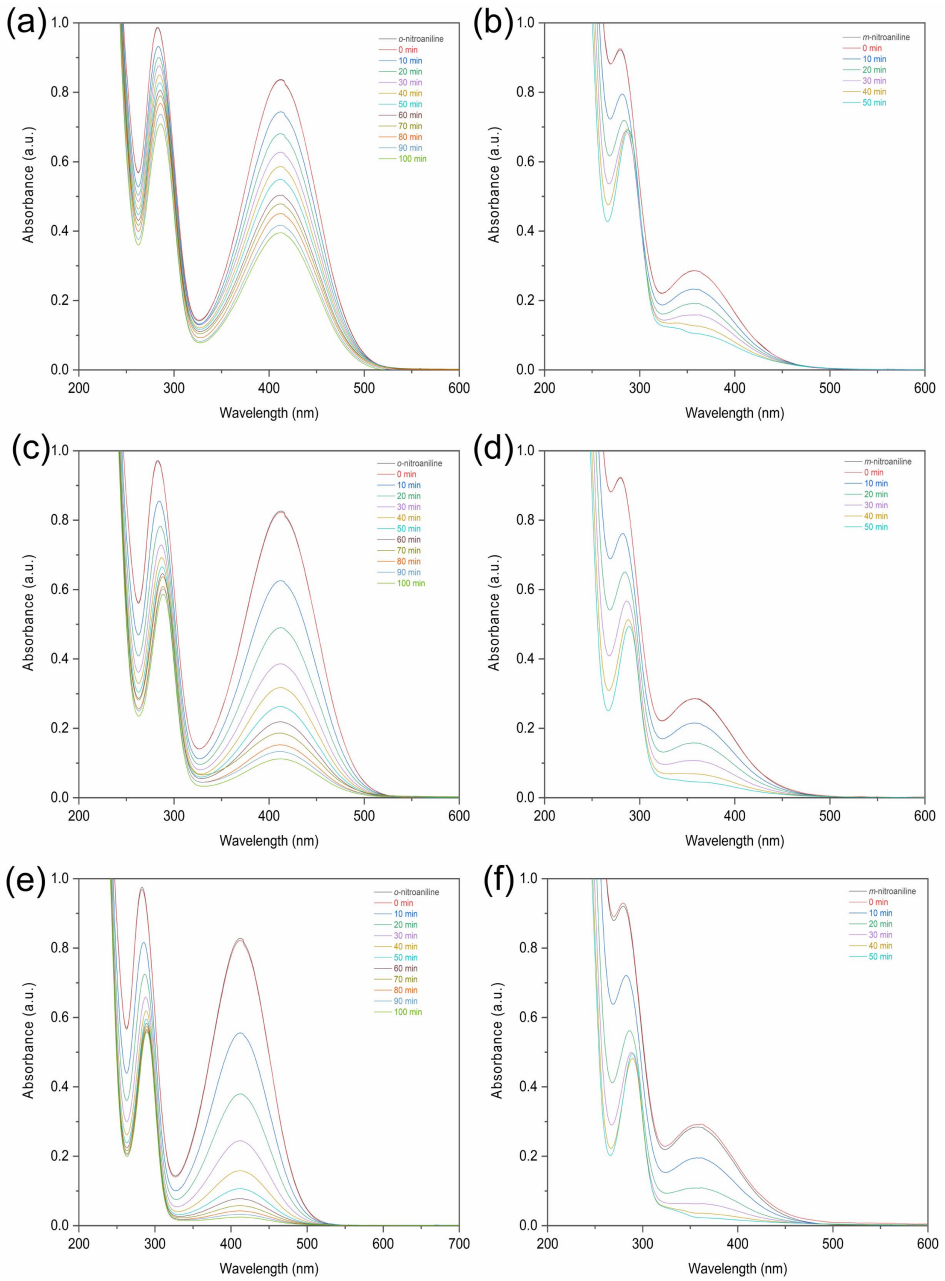

Figure 5. The variation of UV-vis absorption spectra for the reductions of *o*-nitroaniline, *m*-nitroaniline with temperatures at (a-b) 30°C (c-d) 35°C and (e-f) 40°C in the presence of $NaBH_4$ and NiO nanoparticles catalyst.

The reduction rate of *m*-nitroaniline was faster than that of *o*-nitroaniline. *o*-Nitroaniline was stabilized by resonance.[24] However, *m*-nitroaniline is the less stable compare to *o*-nitroaniline as there is no resonance stabilization.[24] Due to the resonance, *o*-nitroaniline was less reactive in the reduction process compare to *m*-nitroaniline.[25,26]

The temperature of the nitroaniline solution is an important parameter in the reduction process. The yield percentage for reduction of *o*-nitroaniline increased from 52.7% to 97.0% as the temperature increases from 303.15 K to 313.15 K (Figure 5a, 5c, 5e, Table 2). The yield percentage for reduction of *m*-nitroaniline increased from 62.7% to 91.9% by increasing temperature from 303.15 K to 313.15 K (Figure 5b, 5e, 5f, Table 2). The reduction processes of nitroaniline were endothermic reactions.

The activation energy of the nitroaniline reductions was calculated using the Arrhenius equation (Figure 6a, 6b).

Table 2. Change in the Catalytic Reduction Rate Constants of *o*-Nitroaniline and *m*-Nitroaniline with Different Temperatures and Activation Parameters in Catalysis with Nickel Oxide Nanoparticles

Compound	Temperature (°C)	k (min^{-1})	R^2 (COD)	E_a (kJ mol^{-1})	ΔH (kJ mol^{-1})	ΔS (J $mol^{-1}K^{-1}$)
o-nitroaniline	30	0.00727	0.99224	125.20	122.74	540.53
	35	0.01953	0.99212			
	45	0.03549	0.99228			
m-nitroaniline	30	0.02010	0.99968	75.09	72.53	384.22
	35	0.03697	0.99696			
	40	0.05197	0.99719			

(Reaction condition: 10 ml [*o*-, *m*-nitroaniline] = 0.0145 mM, [$NaBH_4$] = 13.4 mM, 5mg catalyst.)
*Rate constant (k), coefficient of determination (R^2), activation energy (E_a), enthalpy (ΔH), and entropy (ΔS) for the $NaBH_4$ reduction of *o*-nitroaniline, *m*-nitroaniline at different temperatures using nickel oxide nanoparticles catalyst

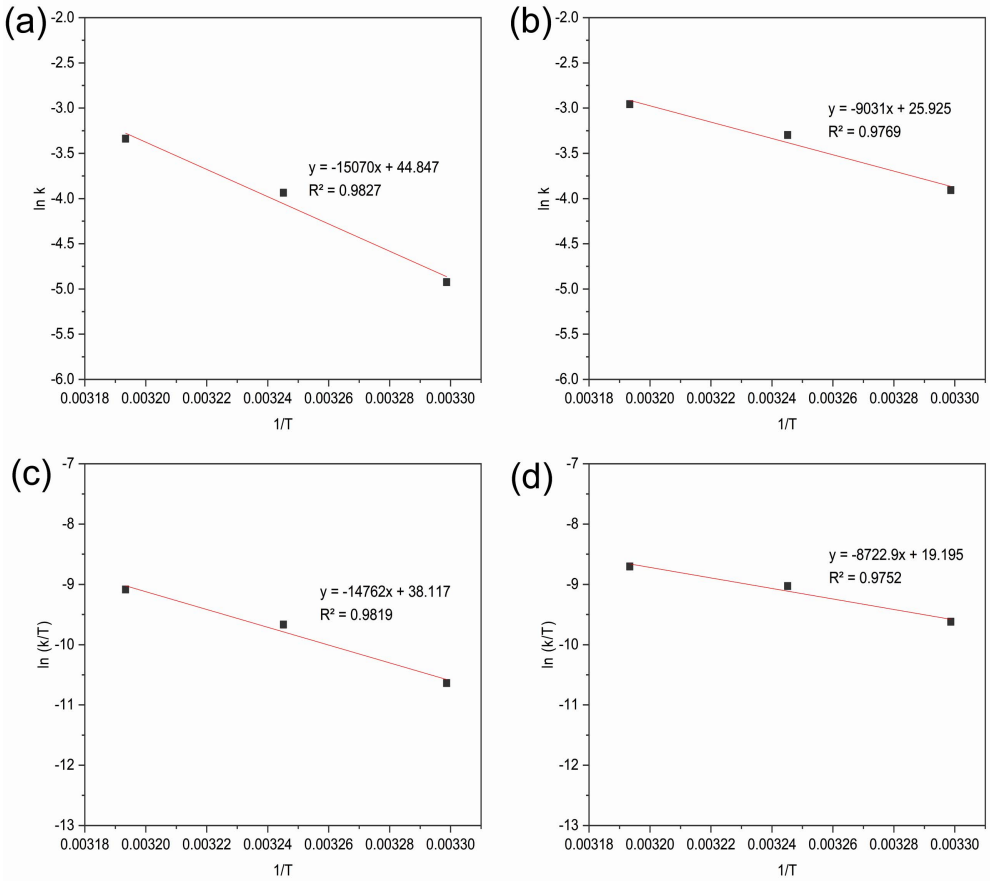

Figure 6. ln$k$ vs 1/T graphs (Arrhenius equation); reduction of (a) *o*-nitroaniline (b) *m*-nitroaniline and ln(k/T) vs 1/T graphs (Eyring equation); reduction of (c) *o*-nitroaniline (d) *m*-nitroaniline using NiO nanoparticles as catalyst with $NaBH_4$ at different temperatures.

$$\ln k = -\frac{E_a}{RT} + \ln A \quad \ldots \quad \textit{Arrhenius equation}$$

where E_a is the activation energy, k is the apparent reaction rate constant, A is the Arrhenius factor, R is the ideal gas constant (8.314 $J \cdot K^{-1} \cdot mol^{-1}$), and T is absolute temperature. The activation energy values for the reduction of *o*-nitroaniline and *m*-nitroaniline were calculated to be 125.20 $kJ \cdot mol^{-1}$ and 75.09 $kJ \cdot mol^{-1}$. The catalytic reduction of *o*-nitroaniline required more activation energy than that of *m*-nitroaniline.[27,28]

Kinetic parameters such as the activation enthalpy (ΔH) and activation entropy (ΔS) were calculated using the Eyring equation (Figure 6c, 6d).

$$\ln\frac{k}{T} = -\frac{\Delta H}{R}\cdot\frac{1}{T} + \ln\frac{\kappa k_B}{h} + \frac{\Delta S}{R} \quad \ldots \text{ Eyring equation}$$

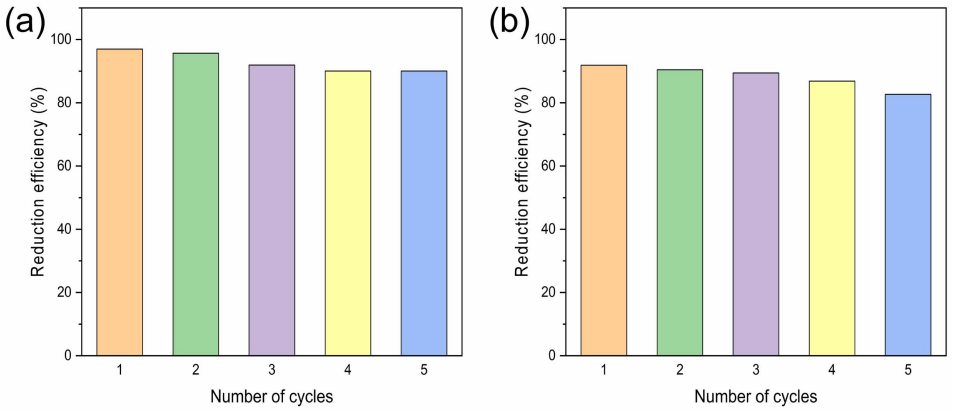

Figure 7. Reusability studies of NiO nanoparticles catalyst for the reduction of (a) *o*-nitroaniline and (b) *m*-nitroaniline.

where k_B is the Boltzmann constant (1.381×10^{-23} J·K^{-1}) and h is the Plank constant (6.626×10^{-34} J·s). In the above Eyring equation, it is assumed that the all species in the transition state proceed to the phenylenediamines, the transmission coefficient ($\kappa = 1$). The activation enthalpy (ΔH) for the reductions of *o*-nitroaniline and *m*-nitroaniline were 122.74 kJ·mol^{-1} and 72.53 kJ·mol^{-1}, from the Eyring equation. The activation entropy (ΔS) for the reductions of *o*-nitroaniline and *m*-nitroaniline were 540.53 J·mol^{-1}·K^{-1} and 384.22 J·mol^{-1}·K^{-1}, from the Eyring equation.[29,30] The reduction of *o*-, *m*-nitroaniline was spontaneous reaction. After the catalytic reduction was finished, the catalyst could be separated through centrifugation. The catalyst was washed several times with deionized water, and reused under same condition.[31,32] The results showed that the catalytic activity of nickel oxide after 5 cycles of the reduction of *o*-nitroaniline and *m*-nitroaniline was decreased slightly from 97.0% to 90.1% and 91.9% to 82.7%, respectively. The catalytic reduction efficiency was decreased due to the loss of catalyst during the washing process.[33] The catalytic activity of the recycled nickel oxide nanoparticles showed good reusability in the reduction of *o*- and *m*-nitroaniline (Figure 7).

Conclusions

The synthesized NiO nanoparticles catalyst was used to reduce *o*- and *m*-nitroanilines in an aqueous solution with $NaBH_4$. At the constant concentrations of $NaBH_4$, nitroaniline, and NiO nanoparticles, *m*-nitroaniline was reduced faster than *o*-nitroaniline. Due to resonance stabilization, *o*-nitroaniline is a more stable than *m*-nitroaniline. After reducing agent of $NaBH_4$, *o*- and *m*-nitroanilines were adsorbed on the surface of the NiO nanoparticles, the reduction process occurred. The kinetics study showed that the reduction of *o*- and *m*-nitroanilines were followed a pseudo first-order reaction rate law. Due to the endothermic reaction, the reduction rate of *o*- and *m*-nitroanilines was enhanced by increasing the temperature.

Acknowledgements

This work was supported by Research Foundation of Sahmyook University in 2019.

References

1. M. T. Amouzadeh, M. Shamsipur, R. Saber and S. Sarkar, U. S. patent 0062185 (2019).
2. K. Zhang, H. Li, X. Xu, and H. Yu, “Synthesis of reduced graphene oxide/NiO nanocomposites for the removal of Cr(VI) from aqueous water by adsorption”, *Microporous Mesoporous Mater.*, **255**, 7 (2018).
3. K. Naseem, R. Begum, and Z. H. Farooqi, “Catalytic reduction of 2-nitroaniline: a review. Environmental Science and Pollution Research”, *Environ. Sci. Pollut. Res.*, **24**, 6446 (2017).
4. D. B. Jirekar, M. Ubale, and M. Farooqui, “Evaluation of Adsorption Capacity of Low-Cost Adsorbent for the Removal of Congo Red Dye from Aqueous Solution”, *Orbital: Electron. J. Chem.*, **8**, 282 (2016).
5. Z. H. Farooqi, K. Naseem, R. Begum, and A. Ijaz, “Catalytic Reduction of 2-Nitroaniline in Aqueous Medium Using Silver Nanoparticles Functionalized Polymer Microgels”, *J. Inorg. Organomet. Polym. Mater.*, **25**, 1554 (2015).
6. A. Aslani, V. Oroojpour, and M. Fallahi, “Sonochemical syn-

thesis, size controlling and gas sensing properties of NiO nanoparticles", *Appl. Surf. Sci.*, **257**, 4056 (2011).
7. V. S. R. Channu, R. Holze, and B. Rambabu, "Synthesis and characterization of NiO nanoparticles for electrochemical applications", *Colloids Surf. A Physicochem. Eng. Asp.*, **414**, 204 (2012).
8. G. Jayakumar, A. A. Irudayaraj, and A. D. Raj, "Photocatalytic Degradation of Methylene Blue by Nickel Oxide Nanoparticles", *Mater. Today: Proc.*, **4**, 11690 (2017).
9. X. Wan, M. Yuan, S. Tie, and S. Lan, "Effects of catalyst characters on the photocatalytic activity and process of NiO nanoparticles in the degradation of methylene blue", *Appl. Surf. Sci*., **277**, 40 (2013).
10. N. N. M. Zorkipli, N. H. H. Kaus, and A. A. Mohamad, "Synthesis of NiO Nanoparticles through Sol-gel Method", *Procedia Chem.,* **19**, 626 (2016).
11. H. Wu, Y. Wang, C. Zheng, J. Zhu, G. Wu, and X. Li, "Multishelled NiO hollow spheres: Easy hydrothermal synthesis and lithium storage performances", *J. Alloys Compd*., **685**, 8 (2016).
12. S. J. Musevi, A. Aslani, H. Motahari, and H. Salimi, "Offer a novel method for size appraise of NiO nanoparticles by PL analysis: Synthesis by sonochemical method", *J. Saudi Chem. Soc*., **20**, 245 (2016).
13. K. Karthik, G. K. Selvan, M. Kanagaraj, S. Arumugam, and N. V. Jaya, "Particle size effect on the magnetic properties of NiO nanoparticles prepared by a precipitation method", *J. Alloys Compd.*, **509**, 181 (2011).
14. K. Anandan and V. Rajendran, "Effects of Mn on the magnetic and optical properties and photocatalytic activities of NiO nanoparticles synthesized via the simple precipitation process", *Mater. Sci. Eng. B*, **199**, 48 (2015).
15. A. C. Gandhi, J. Pant, S. D. Pandit, S. K. Dalimbkar, T. S. Cha, C. L. Cheng, Y. R. Ma, and S. Y. Wu. "Short-Range Magnon Excitation in NiO Nanoparticles", *J. Phys. Chem. C*, **117**, 18666 (2013).
16. H. Ullah, L. Mushtaq, Z. Ullah, M. A. Bangesh, and M. Nawaz, "Cost effective green synthesis of NiO nanostructures as highly efficient photocatalysts for degradation of organic dyes", *Micro Nano Lett.*, **14**, 103 (2019).
17. A. Rahdar, M. Aliahmadb, and Y. Azizib, "NiO Nanoparticles: Synthesis and Characterization", *J. Nanostruct*., **5**, 145 (2015).
18. G. George and S. Anandhan, "Synthesis and characterisation of nickel oxide nanofibre webs with alcohol sensing characteristics", *RSC Adv.*, **4**, 62009 (2014).
19. B. T. Sone, X. G. Fuku, and M. Maaza, "Physical & Electrochemical Properties of Green Synthesized Bunsenite NiO Nanoparticles via Callistemon Viminalis' Extracts", *Int. J. Electrochem. Sci.*, **11**, 8204 (2016).
20. L. Jia, W. Zhang, J. Xu, J. Cao, Z. Xu, and Y. Wang, "Facile Fabrication of Highly Active Magnetic Aminoclay Supported Palladium Nanoparticles for the Room Temperature Catalytic Reduction of Nitrophenol and Nitroanilines", *Nanomaterials*, **8**, 409 (2018).
21. B. Naik, S. Hazra, V. S. Prasad, and N. N. Ghosh, "Synthesis of Ag nanoparticles within the pores of SBA-15: An efficient catalyst for reduction of 4-nitrophenol", *Catal. Commun*., **12**, 1104 (2011).
22. R. Vijayan, S. Joseph, and B. Mathew, "Indigofera tinctoria leaf extract mediated green synthesis of silver and gold nanoparticles and assessment of their anticancer, antimicrobial, antioxidant and catalytic properties", *Artif. Cells Nanomed. Biotechnol*., **46**, 861 (2017).
23. M. A. Bhosale, D. R. Chenna, and B. M. Bhanage, "Ultrasound Assisted Synthesis of Gold Nanoparticles as an Efficient Catalyst for Reduction of Various Nitro Compounds", *Chemistry Select*, **2**, 1225 (2017).
24. T. Aditya, J. Jana, N. K. Singh, A. Pal, and T. Pal, "Remarkable Facet Selective Reduction of 4-Nitrophenol by Morphologically Tailored (111) Faceted Cu_2O Nanocatalyst", *ACS Omega*, **2**, 1968 (2017).
25. J. Sun, Y. Fu, G. He, X. Sun, and X. Wang, "Catalytic hydrogenation of nitrophenols and nitrotoluenes over a palladium/graphene nanocomposite", *Catal. Sci. Technol*., **4**, 1742 (2014).
26. T. Aditya, J. Jana, A. Pal, and T. Pal, "One-Pot Fabrication of Perforated Graphitic Carbon Nitride Nanosheets Decorated with Copper Oxide by Controlled Ammonia and Sulfur Trioxide Release for Enhanced Catalytic Activity", *ACS Omega*, **3**, 9318 (2018).
27. N. Sahiner, S. Sagbas, and N. Aktas, "Very fast catalytic reduction of 4-nitrophenol, methylene blue and eosin Y in natural waters using green chemistry: p(tannic acid)–Cu ionic liquid composites", *RSC Adv.*, **5**, 18183 (2015).
28. N. Sahiner, A. Kaynak, and S. Butun, "Soft hydrogels for dual use: Template for metal nanoparticle synthesis and a reactor in the reduction of nitrophenols", *J. Non. Cryst. Solids*, **358**, 758 (2012).
29. P. Ptáček, F. Šoukal, and T. Opravil, "Introducing the Effective Mass of Activated Complex and the Discussion on the Wave Function of This Instanton", ed by P. Ptáček, F. Šoukal and T. Opravil, p.27-46, IntechOpen Publishers, London, 2018.
30. S. Butun and N. Sahiner, "A versatile hydrogel template for metal nano particle preparation and their use in catalysis", *Polymer*, **52**, 4834 (2011).
31. J. A. Tanna, R. G. Chaudhary, N. V. Gandhare, A.R. Rai, and H. D. Juneja, "Nickel oxide nanoparticles: Synthesis, charac-

terization and recyclable catalyst", *Int. J. Eng. Res*., **6**, 93 (2015).
32. M. A. Nasseri, F. Ahrari, and B. Zakerinasab, "Nickel oxide nanoparticles: a green and recyclable catalytic system for the synthesis of diindolyloxindole derivatives in aqueous medium" *RSC Adv.*, **5**, 13901 (2015).
33. K. H. Liew, T. K. Lee, M. A. Yarmo, K. S. Loh, A. F. Peixoto, C. Freire, and R. M. Yusop, "Ruthenium Supported on Ionically Cross-linked Chitosan-Carrageenan Hybrid $MnFe_2O_4$ Catalysts for 4-Nitrophenol Reduction", *Catalysts*, **9**, 254 (2019).